Case Studies in Thermal Engineering 24 (2021) 100830

Contents lists available at ScienceDirect

Case Studies in Thermal Engineering

journal homepage: http://www.elsevier.com/locate/csite

Condensation risk of exhaust air heat recovery window system: Assessment, key parameters, and prevention measure

Chong Zhang [a,b,*], Jinbo Wang [a], Liao Li [a], Wenjie Gang [a]

[a] Department of Building Environment and Energy Engineering, Huazhong University of Science & Technology, Wuhan, China
[b] Department of Building Services Engineering, The Hong Kong Polytechnic University, Kowloon, Hong Kong, China

ARTICLE INFO

Keywords:
Thermal insulation
Exhaust air heat recovery
Condensation
Building envelope
Window

ABSTRACT

The exhaust air window (EAW) can be regarded as a combination of exhaust air heat recovery unit and window system. The window can locally and directly utilize the exhaust air from each air-conditioned room to reduce the heat loss/gain through window. However, condensation may occur at the internal glazing surface of EAW in winter. To avoid the condensation risk of EAW, some prevention measures were proposed and estimated. In this study, a two-dimensional zonal model of EAW was established to calculate its temperature distribution, and to further identify whether condensation will occur under different boundary conditions. The calculated results were compared with the measured data for verifying the accuracy and reliability of model. A sensitivity analysis was conducted to identify the effects of indoor air temperature and relative humidity, exhaust airflow velocity, and adding a low-e coating on prevention of condensation in winter. The results indicated that adding a low-e coating or decreasing the indoor relative humidity can effectively reduce the critical outdoor temperature of condensation and prevent the occurrence of condensation within the EAW. It was estimated that even under the outdoor air temperature of −20 °C, condensation risk can be avoided by employing a low-e glazing.

1. Introduction

Building sectors have been recognized as a significant portion for reducing the energy consumption and GHG emission [1]. Towards green and sustainable buildings, numerous advanced technologies and methods have been investigated in terms of integrating the renewable energy into buildings [2,3], utilizing the AI or big-data technologies to achieve building operation control and performance prediction [4], improving the thermal insulation of building envelops [5–7], and etc. It was estimated that about 60% of the energy loss of building is resulted from window [8]. Moreover, high-performance window design can potentially contribute to reducing the building energy demand, providing natural lighting, and utilizing solar energy.

Nowadays, many studies mainly focus on reducing the thermal transmittance or controlling the indoor solar heat gain. A lower thermal transmittance can reduce the unwanted conductive heat flux through the window. Advanced window technologies such as the vacuum glazing [9] and aerogel glazing [10] can achieve an extremely low thermal transmittance. Smarts window dynamically modulates its optical properties to utilize the solar heat in winter and block the unwanted incident solar radiation in summer [11]. Integrating the renewable energy with the window systems have been attracting considerable attention in recent years, such as the pipe-embedded window [12], water-flow window [13], and exhaust air window (EAW) [14]. The main purpose of these window

* Corresponding author. Department of Building Services Engineering, The Hong Kong Polytechnic University, Kowloon, Hong Kong, China.
E-mail address: chong0324.zhang@polyu.edu.hk (C. Zhang).

https://doi.org/10.1016/j.csite.2020.100830
Received 31 July 2020; Received in revised form 14 December 2020; Accepted 24 December 2020
Available online 31 December 2020
2214-157X/© 2020 The Author(s). Published by Elsevier Ltd. This is an open access article under the CC BY-NC-ND license (http://creativecommons.org/licenses/by-nc-nd/4.0/).

Nomenclature

C	specific heat, J/(kgK)
D	thickness, m
EAW	exhaust air window
F	view factor
H	height, m
h	heat transfer coefficient, W/(m^{2}K)
I	normal incident solar radiation, W/m^2
L	layer
N	subdivided number of EAW along vertical direction
RH	relative humidity
T	temperature, K
W	width, m
V	volume flow rate, m^3/h
σ	Stefan-Boltzmann's constant
ε	emissivity
α	absorptance
τ	transmittance
ρ	density, kg/m^3

Subscripts

a	air
c	convective heat transfer
g	glass
in	indoor
j	section j
out	outdoor
1	outer layer glass
2	enclosed air channel
3	middle layer glass
4	ventilated air channel
5	inner layer glass

designs is to utilize the low-grade energy sources to reduce the cooling and heating loads of window.

The EAW provides a solution to combine exhaust air heat recovery unit with window system (Fig. 1). It makes the exhaust air from each conditioned room to flow through the channel within window. The airflow exchanges heat with the adjacent glass panes to prevent heat loss in winter and remove the accumulated heat therein in summer [15]. Compared to the air-to-air energy recovery ventilators, this window can directly and locally utilize the exhaust air in each conditioned room instead of adding the additional air-ducts and mechanical fans to gather the exhaust air from different conditioned zones. Currently, numerous studied have been

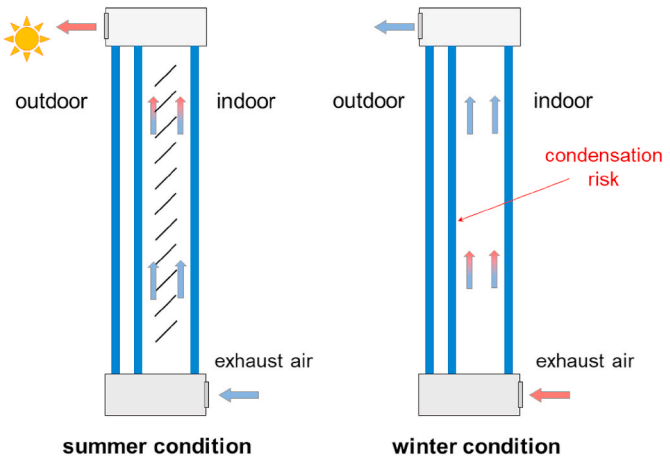

Fig. 1. Structure and principle of EAW.

conducted to investigate the annual thermal/energy performance (including the cooling and heating seasons), estimate the effects of design parameters, and propose the new structures of EAW [14–21].

For the practical application of EAW, however, it should be noticed that condensation may occur at the internal glazing surface that closes to the flowing exhaust air in the heating season, when the temperature of internal glazing surface is below or equal to the dew point temperature of exhaust air. The occurrence of condensation in winter is detrimental to the efficient operation of EAW. Therefore, it is necessary to identify the critical outdoor climate conditions for condensation, estimate the applicability of EAW in winter, and propose the solutions for avoiding the risk of condensation. So far, the above-mentioned issues about the condensation risk of EAW in winter have not been concerned in all the previous studies.

The main objectives of this paper are to identify the critical boundary conditions of condensation, evaluate the influences of key parameters on the prevention of condensation, and propose some methods to reduce the condensation risk of EAW in the heating season. In this study, the theoretical background about the occurrence and prevention of condensation was introduced firstly. Numerical model was developed and validated for calculating the temperature distribution of EAW with given boundary conditions. Some solutions for avoiding the condensation of EAW in the heating season were estimated.

2. Method

2.1. Theoretical background and prevention of condensation

When the interior surface temperature of middle-layer glazing (as shown in Fig. 1) is below or equal to the dew point temperature of its adjacent airflow, condensation will occur on this surface. The dew point temperature is determined by the relative humidity and temperature of air. Meanwhile, the interior surface temperature of middle-layer glazing depends on indoor and outdoor boundary conditions, and structure and design parameters of EAW [21]. The long-term condensation within the EAW in winter may affect the visual quality and heat transfer characteristic of window, increase the pressure drop of exhaust airflow through the air channel, and cause the grown of bacteria.

In order to avoid the condensation within the EAW, the interior surface temperature of middle-layer glazing should be controlled and maintained above the dew point temperature of exhaust air. Temperature gradients of each glazing surface of EAW in vertical direction can be observed [21]. The surface temperature of each glazing gradually decreases from bottom to top in the heating season. Therefore, we compared the interior surface temperature of middle-layer glazing (top part) with the dew point temperature of exhaust air to identify whether condensation will occur.

For the conditioned room, the temperature of exhaust air is approximately equal to the indoor air temperature. Therefore, a lower indoor air temperature and relative humidity will reduce the dew point temperature of exhaust air in the heating season. In this study, the effects of indoor air relative humidity and temperature on the condensation prevention of EAW were investigated. Moreover, increasing the airflow velocity and employing a low-e coating will help to increase the glazing surface temperature. These solutions were also estimated for avoiding the condensation of EAW.

2.2. Mathematical model

Heat transfer processes within the EAW contain natural and forced convection, conduction, long-wave radiation, and solar absorption, reflection, and transmission. Due to the airflow along the vertical direction in air channel, the heat transfer of EAW is two-dimensional. In this study, a two-dimensional zonal model was used to calculate the temperature distribution within the EAW. This model was developed and validated by comparing the calculated results with the measured data in our previous study [22].

Discretization was conducted along the vertical direction to divide the EAW into a series of equal slice, as shown in Fig. 2. Each slice

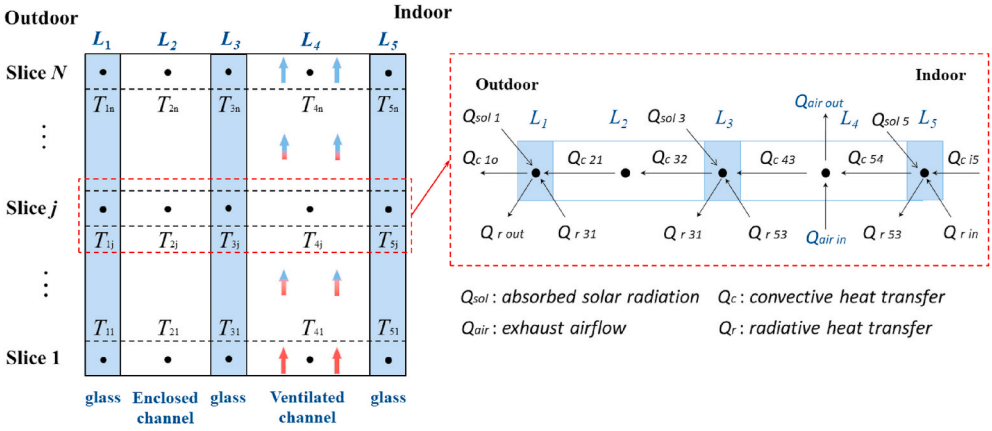

Fig. 2. Schematic discretization of EAW in winter.

contains five subsections including outer layer glazing (L_1), enclosed air channel (L_2), middle layer glazing (L_3), ventilated air channel (L_4), and inner layer glazing (L_5). Therefore, five governing equations for the five subsections from outer layer glazing to inner layer glazing are expressed as follows.

$$h_{co}\left(T_{out}-T_{1j}\right)+\sigma\varepsilon_1\left[\left(T_{sky}^4-T_{1j}^4\right)F_{sky}+\left(T_{ground}^4-T_{1j}^4\right)F_{ground}\right]+h_{c12}\left(T_{2j}-T_{1j}\right)+\frac{\sigma\left(T_{3j}^4-T_{1j}^4\right)}{1/\varepsilon_1+1/\varepsilon_3-1}+I_{sol}\alpha_1=D_g\rho_gC_g\frac{\partial T_{1j}}{\partial t} \tag{1}$$

$$h_{c12}\left(T_{1j}-T_{2j}\right)+h_{c23}\left(T_{3j}-T_{2j}\right)=0 \tag{2}$$

$$h_{c23}\left(T_{2j}-T_{3j}\right)+\frac{\sigma\left(T_{1j}^4-T_{3j}^4\right)}{1/\varepsilon_1+1/\varepsilon_3-1}+h_{c34}\left(T_{4j}-T_{3j}\right)+\frac{\sigma\left(T_{5j}^4-T_{3j}^4\right)}{1/\varepsilon_3+1/\varepsilon_5-1}+I_{sol}\alpha_3=D_g\rho_gC_g\frac{\partial T_{3j}}{\partial t} \tag{3}$$

$$h_{c34}\left(T_{3j}-T_{4j}\right)+h_{c45}\left(T_{5j}-T_{4j}\right)+C_a\rho_aV_a\left(T_{4\cdot j-1}-T_{4j}\right)\frac{N}{HW}=0 \tag{4}$$

$$h_{c45}\left(T_{4j}-T_{5j}\right)+\frac{\sigma\left(T_{3j}^4-T_{5j}^4\right)}{1/\varepsilon_3+1/\varepsilon_5-1}+h_{ci}\left(T_{in}-T_{5j}\right)+\sigma\varepsilon_5\left(T_{in}^4-T_{5j}^4\right)+I_{sol}\alpha_5=D_g\rho_gC_g\frac{\partial T_{5j}}{\partial t} \tag{5}$$

where h_c is convective heat transfer coefficient; I_{sol} is incident solar irradiance; T_{in}, T_{out}, T_{sky}, and T_{ground} are indoor, outdoor, sky, and ground surface temperature, respectively; D is thickness of each layer; ρ and C are density and specific heat, respectively; α is solar absorptance; ε is emissivity of glazing surface; W and H are the width and height of glass pane; V is volume flow rate; σ is the Stefan-Boltzmann's constant; F_{sky} and F_{ground} are view factors between window and sky/ground. The definition of each subscript is described in nomenclature. The calculation methods of above-mentioned convective heat transfer coefficient, sky temperature, and view factors can refer to Ref. [22].

A set of ($N \times 5$) governing equations were proposed for the whole EAW structure. The optical properties of EAW such as the absorptance of each glazing (α_1, α_3, and α_5) were calculated by using the software WINDOW 7.4 [23]. The outdoor temperature, incident solar irradiance, and indoor temperature are the boundary conditions. Iteration algorithm was adopted to solve the proposed equations to obtain the temperatures of all the subsections of EAW. The details of model development are presents in our previous studies [15,22].

2.3. Experimental validation

An experimental platform of EAW was built to validate its numerical model [22]. The schematic of experiment platform is presented in Fig. 3. The EAW prototype used in the experiment consists of three clear glass panes (5 mm). The thickness of each air channel is 40 mm. The air temperature in heat insulation chamber was controlled by air-conditioning. The indoor and outdoor air temperature,

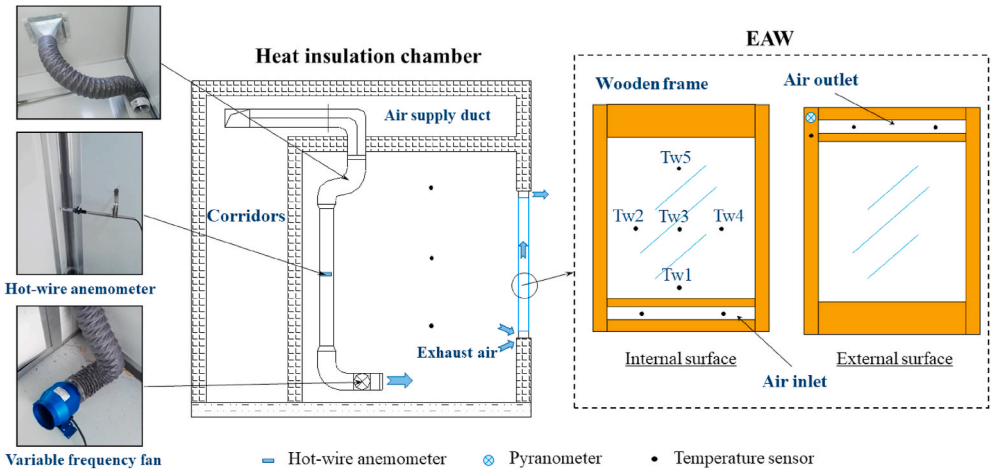

Fig. 3. Schematic of EAW experimental platform.

inlet and outlet air temperature of EAW, interior surface temperature of EAW, incident solar irradiance, and volume flow rate of exhaust air were measured simultaneously with an interval of 1 min.

The measured boundary conditions were the inputs of numerical procedure, and then the calculated data were compared with the measured data to verify the model. The comparison results were presented in Fig. 4. The maximum absolute deviation of the simulated glazing surface temperature for each node was less than 0.4 °C. The root mean squared error (RMSE) values for the temperatures of T_{w1}, T_{w3}, T_{w5}, and outlet air were 0.14 °C, 0.11 °C, 0.1 °C, and 0.34 °C, respectively. This indicates that the proposed model can calculate the glazing surface temperature of EAW with good accuracy and reliability.

3. Results and discussion

A sensitivity analysis was carried out to identify the effects of indoor air temperature and relative humidity, exhaust airflow velocity, and adding a low-e coating on preventing the condensation within EAW in winter. In the case studies, indoor air temperatures (T_{in}) of 18 °C and 20 °C were considered, and relative humidity (RH) ranged from 30% to 50%. Airflow velocity in channel varied from 0.1 m/s to 0.3 m/s. Outdoor air temperature ranged from −20 °C to 10 °C. The EAW consists of a double-glazed unit (two 6 mm clear glass panes with 12 mm air gap) at outside, a 6 mm clear glazing at inside, and an in-between 30 mm ventilated channel. The validated model was adopted to calculate the interior surface temperature of double-glazed unit with different boundary conditions, and to further identify whether condensation will occur in winter.

Fig. 5 shows the calculated interior surface temperature of double-glazed unit with different outdoor air temperatures considering the effects of exhaust air velocity and indoor air temperature. When the interior surface temperature of double-glazed unit is equal to or lower than the dew-point temperature, condensation will occur within the EAW. The dew-point temperature is 9.3 °C for the indoor air conditions of T_{in} = 20 °C and RH = 50% (Fig. 5a). There exists a critical outdoor temperature for the occurrence of condensation within the EAW. It means that condensation within the EAW can be prevented, if the outdoor air temperature is higher than the critical outdoor temperature. Moreover, condensation will occur when the outdoor air temperature is below or equal to this critical temperature. It follows that a lower critical outdoor temperature will reduce the possibility of condensation in winter. The results in Fig. 5a show that the critical outdoor temperature is −1.6 °C for the exhaust air velocity of 0.1 m/s. When this velocity increases to 0.3 m/s, the critical outdoor temperature will decrease from −1.6 °C to −5.1 °C. This means that increasing the exhaust air velocity can help to prevent the condensation within the EAW. Moreover, when the T_{in} decreases from 20 °C to 18 °C, as shown in Fig. 5b, the critical outdoor temperature varies from −1.6 °C to −3.2 °C, but the impact is limited.

The effect of indoor relative humidity on the occurrence of condensation is presented in Fig. 6. The reduction of RH achieves a lower dew-point temperature. Compared to the indoor air conditions of RH = 50%, the dew-point temperature can significantly decrease from 9.3 °C to 6.1 °C and 2.1 °C when the RH reduces to 40% and 30%, respectively. And then the critical outdoor temperature will reduce to −9.0 °C and −18.8 °C for the RH of 40% and 30%, respectively. It follows that no condensation will occur

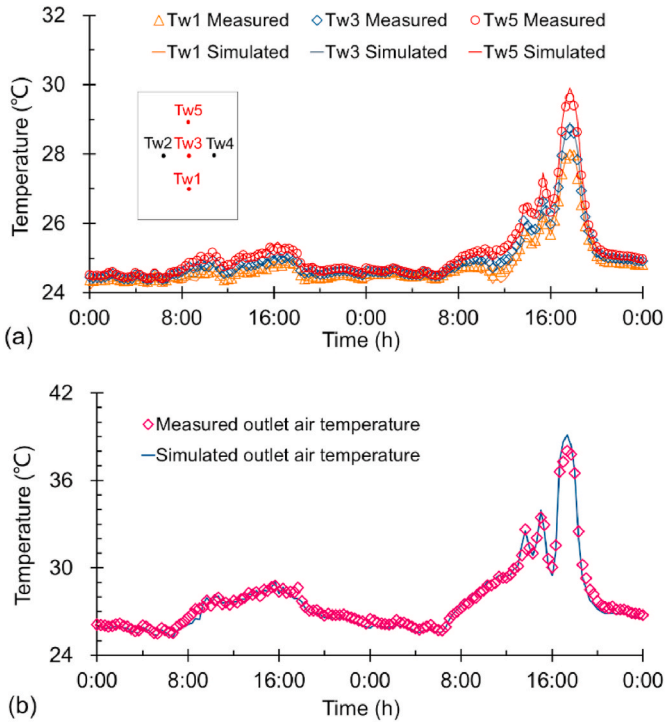

Fig. 4. Comparisons of the simulated and measured: (a) interior surface temperature; (b) outlet air temperature.

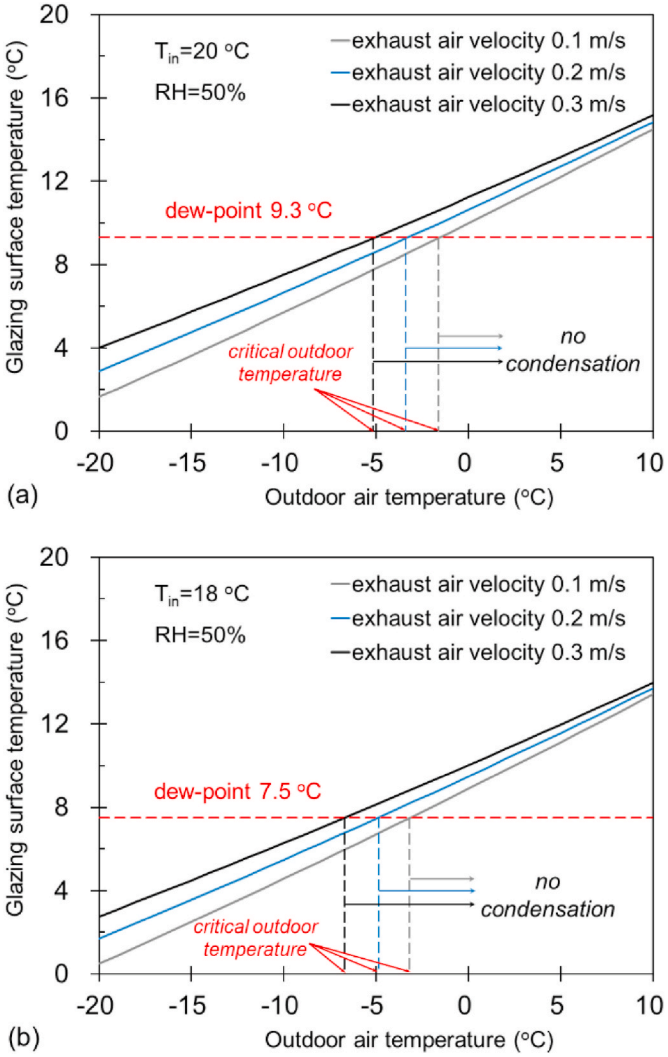

Fig. 5. Effect of exhaust air velocity on the interior surface temperature of double-glazed unit: (a) indoor air temperature 20 °C; (b) indoor air temperature 18 °C.

within the EAW when the outdoor air temperature is higher than −18.8 °C for the indoor air conditions of T_{in} = 20 °C and RH = 30%. For the situation of a lower T_{in}, as shown in Fig. 6b, further reduction of critical outdoor temperature can be achieved. It can be concluded that reducing the indoor air relative humidity can significantly decrease the critical outdoor temperature for the occurrence of condensation within the EAW, and is an effective solution for the prevention of condensation in winter.

Fig. 7 shows the effect of employing a low-e coating on avoiding the occurrence of condensation. In this study, this low-e coating is painted on the exterior surface of middle-layer glazing. The surface emissivity is 0.84 for the conventional clear glazing and 0.141 for the glazing with low-e coating [23]. The calculated results in Fig. 7 reveal that adding a low-e coating can significantly increase the interior surface temperature of double-glazed unit. The interior surface temperature of double-glazed unit is consistently above the dew-point temperature even under the outdoor air temperature of −20 °C, and consequently, the condensation within the EAW can be avoided. For the exhaust air velocity of 0.1 m/s, the critical outdoor temperature can be decrease from −1.6 °C to −20.0 °C by employing a low-e coating. This critical temperature further decreases to −28.7 °C when the velocity increases to 0.3 m/s. Therefore, employing the low-e glazing helps to prevent the condensation of EAW in winter. This critical outdoor temperature of condensation would further decrease by adopting a higher exhaust air velocity or lower indoor air temperature and relative humidity.

4. Conclusions

In this paper, a validated zonal model was adopted to calculate the temperature distribution of EAW, and to identify whether condensation will occur within the EAW under different boundary conditions. Some solutions such as controlling the indoor environment condition, increasing the exhaust air velocity, or adding a low-e coating were proposed. Their impacts on the prevention of

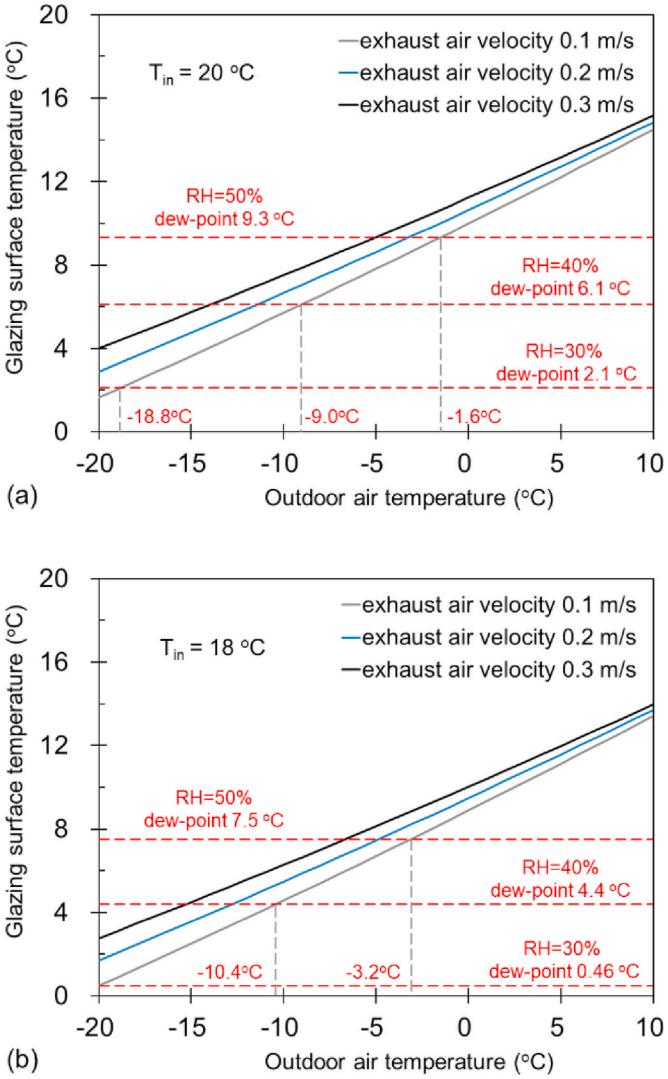

Fig. 6. Effect of indoor relative humidity on preventing the condensation within the EAW: (a) indoor air temperature 20 °C; (b) indoor air temperature 18 °C.

condensation were further estimated. For an indoor environment condition of $T_{in} = 20$ °C and RH = 50%, condensation occurs within the EAW in winter when the outdoor air temperature is below or equal to −1.6 °C. This means that there is a high possibility of condensation for cold weather conditions. The results of case studies indicate that employing a low-e glazing or decreasing the indoor relative humidity can effectively decrease the critical outdoor temperature for the occurrence of condensation, which is beneficial to avoid the condensation risk and enhance the applicability of EAW in cold climatic conditions. Controlling the indoor temperature or exhaust air velocity helps to reduce the possibility of condensation, but the impact is not significant. The critical outdoor temperature for the occurrence of condensation can be decreased to −20 °C by employing a low-e glazing instead of conventional clear glazing.

CRediT authorship contribution statement

Chong Zhang: Methodology, Investigation, Formal analysis, Funding acquisition, Visualization, Writing-original draft preparation, Writing-review and editing. **Jinbo Wang:** Conceptualization, Supervision. **Liao Li:** Data curation. **Wenjie Gang:** Software, Validation.

Declaration of competing interest

The authors declare that they have no known competing financial interests or personal relationships that could have appeared to influence the work reported in this paper.

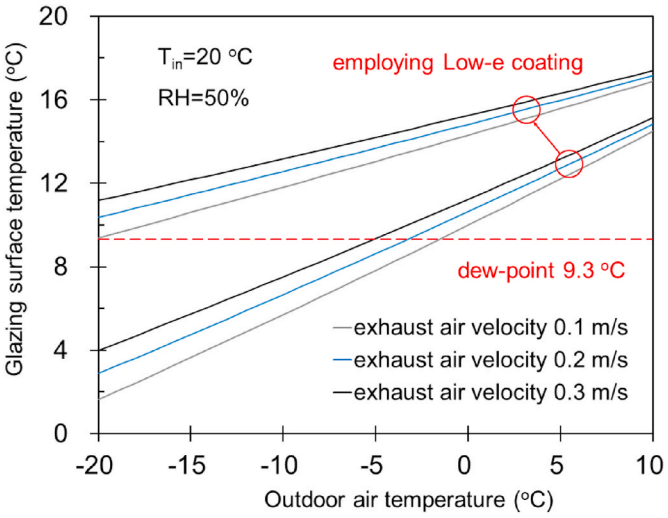

Fig. 7. Effect of employing a low-e coating on the interior surface temperature of double-glazed unit.

Acknowledgement

This work is supported by the National Natural Science Foundation of China (No. 51808239), and the Hong Kong Scholars Program (No. XJ2019044).

References

[1] J.S. Li, H.W. Zhou, J. Meng, Q. Yang, B. Chen, Y.Y. Zhang, Carbon emissions and their drivers for a typical urban economy from multiple perspectives: a case analysis for Beijing city, Appl. Energy 226 (2018) 1076–1086.
[2] C. Zhang, C.L. Cui, Y. Zhang, J.Q. Yuan, Y.M. Luo, W.J. Gang, A review of renewable energy assessment methods in green building and green neighborhood rating systems, Energy Build. 195 (2019) 68–81.
[3] C. Zhang, J.B. Wang, L. Li, F.F. Wang, W.J. Gang, Utilization of earth-to-air heat exchanger to pre-cool/heat ventilation air and its annual energy performance evaluation: A case study, Sustainability 12 (2020), 8330.
[4] C. Fan, F. Xiao, Y. Zhao, A short-term building cooling load prediction method using deep learning algorithms, Appl. Energy 195 (2017) 222–233.
[5] M. Khoukhi, A. Hassan, S. Abdelbaqi, The impact of employing insulation with variant thermal conductivity on the thermal performance of buildings in the extremely hot climate, Case Stud. Therm. Eng. 16 (2019) 100562.
[6] M. Khoukhi, S. Abdelbaqi, A. Hassan, Transient temperature change within a wall embedded insulation with variable thermal conductivity, Case Stud. Therm. Eng. 20 (2020) 100645.
[7] C. Zhang, W.J. Gang, X.H. Xu, L. Li, J.B. Wang, Modelling, experimental test, and design of an active air permeable wall by utilizing the low-grade exhaust air, Appl. Energy 240 (2019) 730–743.
[8] B.P. Jelle, A. Hynd, A. Gustavsen, D. Arasteh, H. Goudey, R. Hart, Fenestration of today and tomorrow: a state-of-the-art review and future research opportunities, Sol. Energy Mater. Sol. Cells 96 (2012) 1–28.
[9] H. Son, T.H. Song, Heat transfer and stress distribution in the central part of vacuum glazing, Appl. Therm. Eng. 159 (2019) 113926.
[10] Y.J. Lv, H.J. Wu, Y.C. Liu, Y. Huang, T. Xu, X.Q. Zhou, R.D. Huang, Quantitative research on the influence of particle size and filling thickness on aerogel glazing performance, Energy Build. 174 (2018) 190–198.
[11] M. Aburas, V. Soebarto, T. Williamson, R.Q. Liang, H. Ebendorff-Heidepriem, Y.P. Wu, Thermochromic smart window technologies for building application: a review, Appl. Energy 255 (2019) 113522.
[12] S. Yan, X.T. Li, B.L. Wang, W.X. Shi, W.H. Lyu, A method to describe the thermal property of pipe-embedded double-skin façade: equivalent glass window, Energy Build. 195 (2019) 33–44.
[13] Y.L. Lyu, W.J. Liu, H. Su, X. Wu, Numerical analysis on the advantages of evacuated gap insulation of vacuum-water flow window in building energy saving under various climates, Energy 175 (2019) 353–364.
[14] F. Khalvati, A. Omidvar, Summer study on thermal performance of an exhausting airflow window in evaporatively-cooled buildings, Appl. Therm. Eng. 153 (2019) 147–158.
[15] C. Zhang, J.B. Wang, X.H. Xu, F.X. Zou, J.H. Yu, Modeling and thermal performance evaluation of a switchable triple glazing exhaust air window, Appl. Therm. Eng. 92 (2016) 8–17.
[16] K.H. Haddad, A.H. Elmahdy, Comparison of the monthly thermal performance of an exhaust-air window and a supply-air window, ASHRAE Trans 105 (1999) 918–926.
[17] D. Saelens, J. Carmeliet, H. Hens, Energy performance assessment of multiple-skin facades, HVAC R Res. 9 (2003) 167–185.
[18] Y. Takemasa, S. Togari, K. Miura, M. Katoh, M. Hiraoka, J. Owada, Evaluation of calculation models for predicting thermal performance of various window systems, ASHRAE Trans 119 (2013) 1–20.
[19] M.C. Skaff, L. Gosselin, Summer performance of ventilated windows with absorbing or smart glazings, Sol. Energy 105 (2014) 2–13.
[20] M.H. Kim, C.Y. Oh, J.H. Hwang, H.W. Choi, W.J. Yang, Thermal performance of the exhausting and the semi-exhausting triple-glazed airflow windows, Int. J. Energy Res. 30 (2006) 177–190.
[21] C. Zhang, W.J. Gang, J.B. Wang, X.H. Xu, Q.Z. Du, Experimental investigation and dynamic modeling of a triple-glazed exhaust air window with built-in Venetian blinds in the cooling season, Appl. Therm. Eng. 140 (2018) 73–85.
[22] C. Zhang, W.J. Gang, J.B. Wang, X.H. Xu, Q.Z. Du, Numerical and experimental study on the thermal performance improvement of a triple glazed window by utilizing low-grade exhaust air, Energy 167 (2019) 1132–1143.
[23] US Department of Energy, Lawrence berkeley national laboratory. WINDOW 7.4. https://windows.lbl.gov/software/window.